

Tunable Charge Density Wave Transport in a Current-Effect Transistor

N. Marković, M. A. H. Dohmen, and H. S. J. van der Zant
Department of Applied Physics and DIMES, Delft University of Technology,
Lorentzweg 1, 2628 CJ Delft,
The Netherlands
(June 29, 1999)

The collective charge density wave (CDW) conduction is modulated by a transverse single-particle current in a transistor-like device. Nonequilibrium conditions in this geometry lead to an exponential reduction of the depinning threshold, allowing the CDWs to slide for much lower bias fields. The results are in excellent agreement with a recently proposed dynamical model in which "wrinkles" in the CDW wavefronts are "ironed" by the transverse current. The experiment might have important implications for other driven periodic media, such as moving vortex lattices or "striped phases" in high- T_c superconductors.

PACS numbers: 71.45.Lr, 71.45.-d, 72.15.Nj

The charge-density-wave (CDW) state, characterized by a periodic modulation of the conduction electron density, is commonly observed in low-dimensional conductors [1]. It is found to be the ground state in various inorganic and organic materials with a chain-like structure, giving rise to remarkable electrical properties [2–4]. Similar charge-ordered states ("striped phases") play an important role in high- T_c superconductors [5] and two-dimensional electron gases in the quantum Hall regime [6].

A particularly interesting feature of the CDW state is its collective transport mode, very similar to superconductivity [7]: under an applied electric field, the CDWs slide along the crystal, giving rise to a strongly nonlinear conductivity. Since even a small amount of disorder pins the CDWs, sliding occurs only when the applied electric field exceeds a certain threshold field. The pinning mechanisms, the onset of collective motion and the dynamics of a moving CDW are typical characteristics of the complex physics which describes a very general class of disordered periodic media [8–15]. These include a wide variety of periodic systems, as diverse as vortex lattices in superconductors and Josephson junction arrays [16–18], Wigner crystals [19], colloids [20], magnetic bubble arrays [21] and models of mechanical friction [22].

The focus of recent theoretical and experimental research on disordered periodic media have been their *nonequilibrium* dynamical properties. One of the issues that have been raised is the effect of a single-particle current, due to uncondensed electrons and quasiparticle excitations. In a recent theoretical work, Radzihovsky and Toner [26] discovered that a single-particle current has the most profound effects when it flows perpendicular to the CDW sliding direction. Based on general symmetry

principles, this leads to nonequilibrium CDW dynamics even if CDW itself is stationary. Here we report our study of the CDW transport in the presence of such a transverse single-particle current. We find that the sliding CDW motion is stable against a small transverse current, but large currents have a dramatic effect: the longitudinal depinning threshold field is exponentially reduced for the normal current densities which exceed some crossover value J_c . In other words, the collective longitudinal current is *enhanced* by the transverse single-particle current. The characteristics of this *current-effect* transistor are in excellent agreement with the predictions of Radzihovsky and Toner [26].

The experiments were carried out on single crystals of NbSe_3 . This material has a very anisotropic, chain-like structure [2]. It exhibits two CDW transitions, each involving different types of chains, at $T_P = 145\text{K}$ and $T_P = 59\text{K}$. A small portion of the conduction electrons remains uncondensed, providing a metallic single-particle channel.

A single crystal of dimensions $2.7\text{ mm} \times 36\ \mu\text{m} \times 240\ \mu\text{m}$ was glued onto a sapphire substrate. A pattern of gold contacts was then defined on top of it using electron-beam lithography. The pattern consisted of two current leads at two ends of the crystal, and a row of devices, each with two transverse current leads and two voltage leads. A scheme of such a transistor device is shown in the inset of Fig. 1.

The transverse current leads were $5\text{--}100\ \mu\text{m}$ wide, and overlapped the crystal by $1\text{--}5\ \mu\text{m}$. To ensure contact on both sides of the crystal, $180\ \text{nm}$ thick layer of gold was evaporated at angles of 45 degrees with respect to the substrate, as well as perpendicular to it. The contact resistance of the transverse leads was by $1\text{--}2$ orders of magnitude larger than the resistance of the crystal in the longitudinal direction, which precludes considerable shunting of the current through the transverse leads. A dc current of up to $1\ \text{mA}$ was injected at the transverse leads. The transverse leads were not electrically connected to the longitudinal circuit, except through the crystal. Since the CDWs can only slide in the longitudinal direction, the transverse current is due to single electrons.

The longitudinal current was injected at the two far ends of the crystal. The voltage leads were $180\ \text{nm}$ thick, $5\ \mu\text{m}$ wide and the spacing between them was $50\text{--}500\ \mu\text{m}$. The longitudinal current-voltage characteristics and the differential resistance were studied as a function of trans-

verse current at different temperatures, ranging from 25-120 K.

The current-voltage characteristics for one of the devices are shown on Fig. 1. In the absence of the transverse current, the CDWs are pinned at low bias voltages. The I-V is linear, as the current is due to uncondensed electrons and quasiparticles that are thermally excited above the CDW gap. When the applied voltage reaches the threshold value $V_T(I_x = 0)$, marked by an arrow in Fig. 1, the CDWs are depinned and start to slide. A sharp increase in current is observed at V_T due to this additional conduction channel.

When a transverse current I_x is applied, V_T decreases and the sliding starts at lower bias voltages. Thus, CDWs that were pinned for $J_x = 0$, start sliding at lower fields when a transverse current is applied. A new linear regime sets in at low bias voltages, where $V_T < V_T(I_x = 0)$. The resistance in this regime is lower than the single particle contribution R at $J_x = 0$. This makes the effect easily distinguishable from heating: since most of the measurements were carried out at the temperatures at which $dR/dT > 0$, heating would result in a higher single-particle resistance.

The threshold field reduction is more strikingly visible in the differential resistance measurements, shown in Fig. 2. The differential resistance at low bias fields, due to uncondensed electrons and excited quasiparticles, is mostly unaffected by the transverse current. The onset of CDW sliding, characterized by a sharp drop in differential resistance, is shifted towards zero as I_x is increased. The same reduction of the threshold field is also observed for negative bias voltages and the plots are nearly symmetric around $V = 0$. We have found no differences when changing the sign of either the longitudinal current or the transverse current.

The reduction of the sliding threshold does not occur for arbitrarily small transverse currents. The dependence of the threshold field E_T on the transverse current density J_x for two samples [27] is shown in Fig. 3. It is evident that E_T remains unchanged until J_x reaches some crossover value J_c . For $J_x > J_c$, E_T decreases with increasing J_c . The transverse current density dependence of the threshold field E_T for $J_x > J_c$ can be fit by:

$$E_T(J_x) = E_T(0) \frac{J_x}{J_c} \exp\left(1 - \frac{J_x}{J_c}\right) \quad (1)$$

where $E_T(0)$ is the threshold field at $J_x = 0$. Once the crossover value of the transverse current J_c is exceeded, the depinning threshold field decreases and the CDW conduction channel is activated by much lower bias voltages.

The observation of a crossover current J_c rules out the possibility that the threshold field reduction is due to current inhomogeneities around the transverse contacts. If the changes in E_T were due to a longitudinal component of an inhomogeneous transverse current, then such changes would be apparent at any value of J_x , and no J_c

would be observed. Furthermore, it is not clear that such inhomogeneities would lead to the observed exponential reduction of E_T .

The exponential decrease of the threshold field described by Eq. 1. has recently been predicted by Radzihovsky and Toner [26]. In their model, the value of the crossover current density J_c needed for the initial suppression of E_T is expected to be proportional to the value of the threshold field at $J_x = 0$, and is given by [26]:

$$J_c \propto \sigma_0 E_T(0) (\xi_L k_F) (\rho_n / \rho_{CDW}) \quad (2)$$

where σ_0 is the conductivity at very high bias fields, k_F the Fermi wave vector and ρ_n and ρ_{CDW} are normal and CDW electron densities, respectively. The correlation length ξ_L [8,28] is a measure for the coherence in the sample and decreases with increasing disorder.

E_T is known to be temperature dependent, following $E_T = E_T(0)e^{-T/T_0}$ [29], where T is the temperature, and T_0 is a constant. The dependence of J_c on $E_T(0)$ can therefore be studied by measuring at different temperatures. The dependence of J_c on $\sigma_0 E_T(0)$ is shown in the inset of Fig. 3: J_c grows linearly with $\sigma_0 E_T(0)$ and it extrapolates to zero for $E_T(0) = 0$. The crossover current densities of $10^3 - 10^4$ A/cm² estimated from Eq. 2. [26] are in excellent agreement with the values measured in our experiment.

We have shown that the conduction in the CDW channel can be enhanced by a single-particle current flowing transversely to the CDW sliding direction. This surprising behavior has been observed in samples with different geometries, at different temperatures, and in both CDW regimes of NbSe₃, suggesting that it is a general property of the CDW transport.

The dynamical model of Radzihovsky and Toner [26] provides a physical origin of this effect: the CDWs become more ordered due to momentum transfer with transversely moving normal carriers. This mechanism is illustrated in Fig. 4. In the absence of defects, the charge density wave fronts are straight and parallel to each other (left side of the picture). The single-particle transverse current, marked by "a" on Fig. 4, can flow with little or no interaction with the CDW. In the presence of defects or impurities in the crystal, the CDW deforms to lower its energy and the wavefronts are "wrinkled" (right side of the picture). In this case, the transversely moving electrons ("b") are more likely to be deflected. The conservation of linear momentum results in a reaction force back on the CDW. This way the CDW roughness is reduced as the CDW wavefronts are straightened out or "ironed" by the transverse current. The CDW transport across the sample is therefore more coherent and less susceptible to pinning. The lower pinning strength then leads to a lower threshold field.

Since the conduction in the CDW channel can be modulated by a current in the single particle channel, this device in principle works as a transistor, raising a question of a possible practical application. The maximum gain

observed in our experiments was $\Delta I/I_x = 0.15$. A simple estimate from our measurements suggests that the maximum gain is proportional to ξ_L^{-1} . The gain can therefore be improved by using dirtier crystals or smaller samples in which ξ_L is limited by the sample sizes.

Apart from being intriguing in their own right as an important test of the theory, our results may provide a useful insight into related phenomena which are much more difficult to study experimentally. As mentioned above, this novel effect is relevant to a variety of other periodic systems which share the same symmetries and a similar geometry. A particularly interesting example might be the "striped phases" in superconducting oxides, whose role in high- T_c superconductivity is still not resolved.

The authors are grateful to Yu. Latyshev and P. Monceau for providing the crystal, and to L. Radzihovsky, Yu. Nazarov and S. Zaitsev-Zotov for useful discussions. This work was supported by the Netherlands Foundation for Fundamental Research on Matter (FOM). HSJvdZ was supported by the Dutch Royal Academy of Arts and Sciences (KNAW).

[1] R. E. Peierls, *Ann. Phys. Leipzig* **4**, 121 (1930).
[2] For a review, see G. Grüner, *Density Waves in Solids*, Addison-Wesley (1994).
[3] G. Grüner, *Rev. Mod. Phys.* **60**, 1129 (1988).
[4] R. E. Thorne, *Physics Today*, 42 (May 1996).
[5] S. A. Kivelson, E. Fradkin, and V. J. Emery, *Nature* **393**, 550 (1998); J. M. Tranquada, B. J. Sternlieb, J. D. Axe, Y. Nakamura, and S. Uchida, *Nature* **375**, 561 (1995).
[6] A. A. Koulakov, M. M. Fogler, and B. I. Shklovskii, *Phys. Rev. Lett.* **76**, 499 (1996).
[7] H. Fröhlich, *Proc. R. Soc. A* **223**, 296 (1954).
[8] H. Fukuyama and P. A. Lee, *Phys. Rev. B* **17**, 535 (1978); P. A. Lee and T. M. Rice, *Phys. Rev. B* **19**, 3970 (1979).
[9] J. Bardeen, *Phys. Rev. Lett.* **42**, 1498 (1979); *ibid.* **45**, 1978 (1980).
[10] L. Sneddon, M. C. Cross, and D. S. Fisher, *Phys. Rev. Lett.* **49**, 292 (1982).
[11] S. Scheidl and V. M. Vinokur, *Phys. Rev. E* **57**, 2574 (1998).
[12] T. Giamarchi and P. Le Doussal, *Phys. Rev. Lett.* **76**, 3408 (1996).
[13] L. Balents and M. P. A. Fisher, *Phys. Rev. Lett.* **75**, 4270 (1995).
[14] L. Balents, M. C. Marchetti, and L. Radzihovsky, *Phys. Rev. Lett.* **78**, 751 (1997); *Phys. Rev. B* **57**, 7705 (1998).
[15] V. M. Vinokur and T. Natterman, *Phys. Rev. Lett.* **79**, 3471 (1997).
[16] G. Blatter, M. V. Feigel'man, V. B. Geshkenbein, A. I. Larkin, and V. M. Vinokur, *Rev. Mod. Phys.* **66**, 1125 (1994).
[17] C. Reichhardt, C. J. Olson, and F. Nori, *Phys. Rev. B* **58**, 6534 (1998), and references therein.

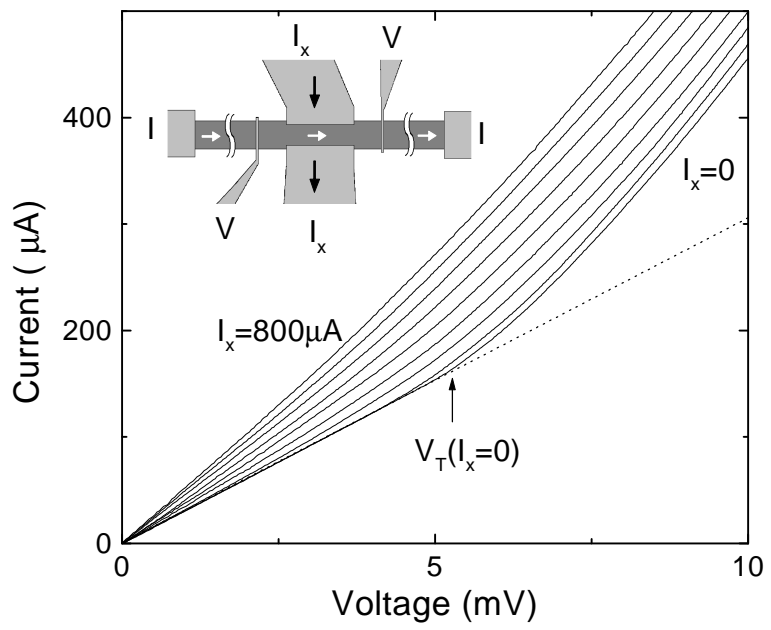
[18] A. M. Troyanovski, J. Aarts, and P. H. Kes, *Nature* **399**, 665 (1999).
[19] M.-C. Cha and H. Fertig, *Phys. Rev. B* **50**, 14 368 (1994).
[20] J. Chakrabarti, H. R. Krishnamurti, A. K. Sood, and S. Sengupta, *Phys. Rev. Lett.* **75**, 2232 (1995).
[21] J. Hu and R. M. Westervelt, *Phys. Rev. B* **51**, 17 279 (1995).
[22] O. M. Braun, A. R. Bishop, and J. Röder, *Phys. Rev. Lett.* **79**, 3692 (1997); *ibid.* **82**, 3097 (1999).
[23] M. Hayashi and H. Yoshioka, *Phys. Rev. Lett.* **77**, 3403 (1996).
[24] A. Melikidze, *Phys. Rev. B* **58**, 13 534 (1998).
[25] T. L. Adelman, S. V. Zaitsev-Zotov, and R. E. Thorne, *Phys. Rev. Lett.* **74**, 5264 (1995).
[26] L. Radzihovsky and J. Toner, *Phys. Rev. Lett.* **81**, 3711 (1998).
[27] In the x -axis, the data of the 100 μm device have been scaled by a factor 0.7. This factor can be understood from the anisotropy of NbSe_3 . Depending on temperature, the resistance perpendicular to the CDW chains (but still in plane) is a factor 10-20 higher than in the chain direction (N.P. Ong and J.W. Brill, *Phys. Rev. B* **18** (1978) 5265). This means that on both sides of the the transverse leads current spreads out over a distance $\sim 4W$, where W is the crystal width. Note that in Fig. 3, J_x is calculated without correcting for the anisotropy of the current.
[28] A. Larkin, *Sov. Phys. JETP* **31**, 784 (1970).
[29] J. McCarten, D. A. DiCarlo, M. P. Maher, T. L. Adelman, and R. E. Thorne, *Phys. Rev. B* **46**, 4456 (1992).

FIG. 1. Current-voltage characteristics for a 36 μm wide and 0.24 μm thick NbSe_3 crystal at 45 K with the values of the transverse current ranging from 0 (bottom) up to 800 μA (top). The width of the transverse current leads was 100 μm , and the spacing between the voltage leads was 225 μm . The dotted line represents the Ohmic behavior of the uncondensed electrons. The data deviate from that line when the charge density waves are depinned and start to slide, contributing additional current. The depinning threshold V_T , marked by an arrow, decreases when a transverse current I_x is applied. Inset: The scheme of the transistor-like device, which consists of the crystal (dark shaded area) and six gold leads (light shaded areas): I for the longitudinal current, which is injected at the far ends of the crystal, V for voltage measurements and I_x for the transverse current injection.

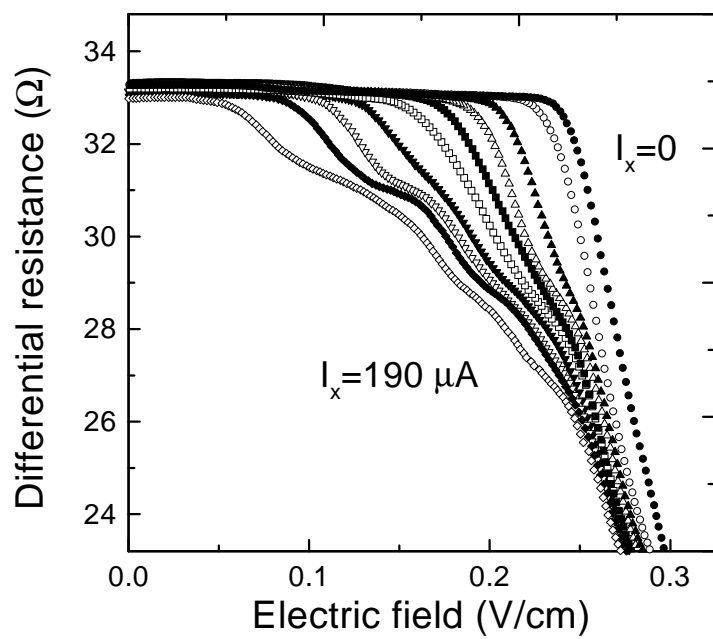
FIG. 2. Differential resistance as a function of electric field at 45 K of the same device as in Fig. 1. Different symbols represent different values of the transverse current I_x , ranging from 0 (filled circles) to 190 μA (filled squares). The threshold field at which the differential resistance drops due to the depinning of the charge density waves is shifted to lower values as the transverse current is increased.

FIG. 3. Depinning threshold field E_T , scaled by its value at $J_x=0$, as a function of transverse current density J_x at 55 K for two different devices. The widths of the transverse current leads were 100 μm (circles) and 30 μm (triangles). The solid line represents a fit to Eq. 1. Inset: The crossover transverse current density J_c needed for the initial suppression of the depinning threshold E_T increases with the value of E_T at $J_x=0$. J_c is plotted here as a function of $\sigma_0 E_T(0)$ for comparison with Eq. 2, where σ_0 is the conductance at bias fields much larger than E_T . Each data point was determined at a different temperature: from right to left, the temperatures were 25, 30, 35, 40, 45, 50 and 55 K.

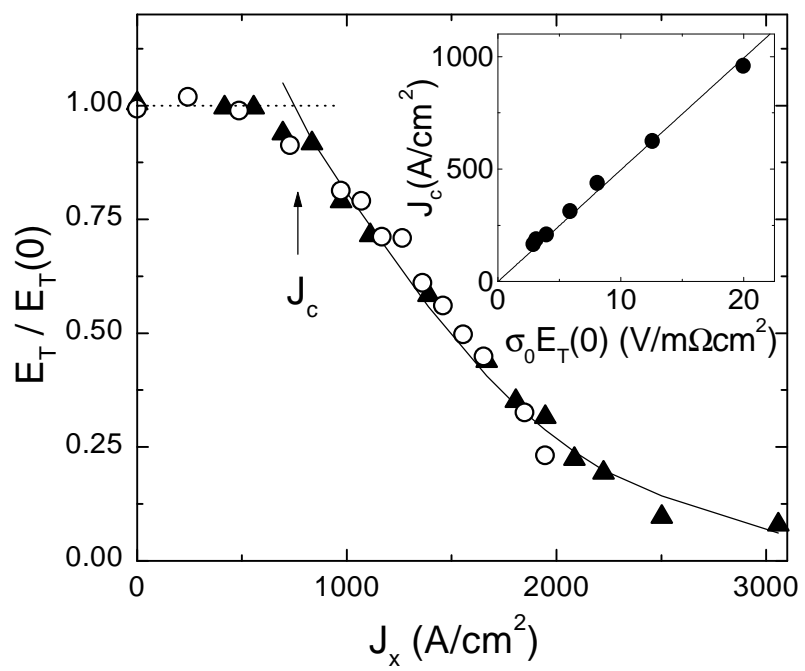
FIG. 4. Dynamical model for the threshold field reduction: the vertical lines represent the charge density wavefronts which, if depinned, can move in the horizontal direction. The large filled circles represent the impurities or other defects in the crystal. The CDW sliding direction and the transverse current direction are indicated by the arrows. The small open circles ("a" and "b") represent the transverse single particle current. The deformations of the wavefronts due to momentum transfer with the transverse current are shown by the dotted lines.



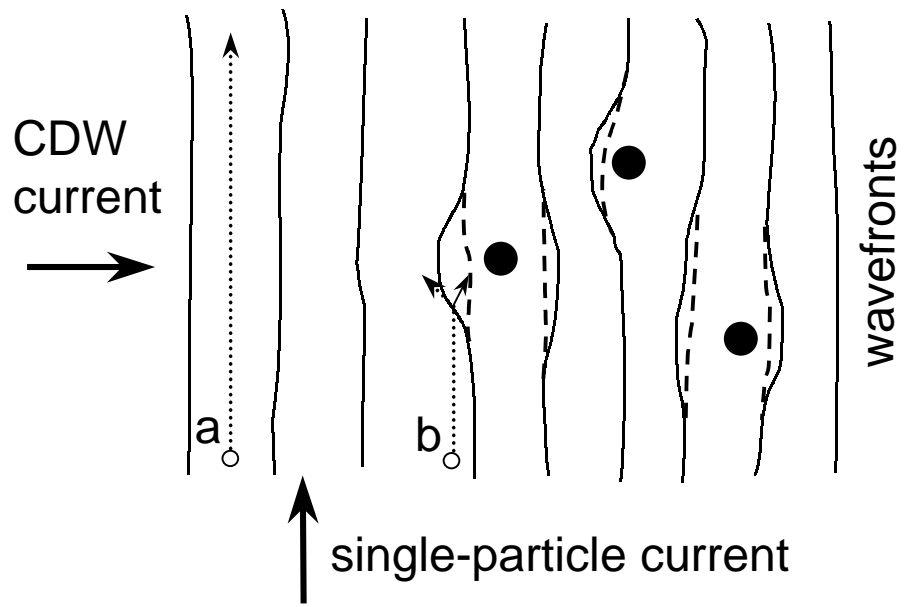
N. Markovic *et al*, Figure 1



N. Markovic *et al*, Figure 2



N. Markovic *et al*, Figure 3



N. Markovic *et al*, Figure 4